Open Access

Catalysis Research

LIDSEN Publishing Inc.

Original Research

Tungstophosphate Intercalated ZnAl Layered Double Hydroxide for Adsorptive and Visible Light Driven Photocatalytic Decolourisation of Organic Dyes

Bhabani Shankar Mohanta [1, ‡], Rita Das [2, *], Nigamananda Das [1]

1. Department of Chemistry, Utkal University, Bhubaneswar – 751 004, India; E-Mails: bhabanibetonoti@gmail.com; dasn.chem@utkaluniversity.ac.in
2. Department of Chemistry, B.J.B. Autonomous College, Bhubaneswar 751 014, India; E-Mail: rita.chem2010@gmail.com

‡ Current Affiliation: Department of Chemistry, Maharaja Sriram Chandra Bhanja Deo University, Baripada 757 003, Odisha, India

* **Correspondence:** Rita Das; E-Mail: rita.chem2010@gmail.com

Academic Editor: Narendra Kumar

Catalysis Research
2023, volume 3, issue 4
doi:10.21926/cr.2304025

Received: December 21, 2022
Accepted: September 18, 2023
Published: October 13, 2023

Abstract

Tungstophosphate ($PW_{12}O_{40}^{3-}$) intercalated ZnAl-Layered double hydroxide (ZnAl-PW_{12}) was successfully synthesized through the rehydration of calcined LDH. Chemical analyses and characterizations by powder XRD, FT-IR, and Diffuse reflectance UV-Vis spectra confirmed the intercalation of $PW_{12}O_{40}^{3-}$ ions equivalent to ~80% of the residual positive charge in the brucite layer. The efficiency of ZnAl-PW_{12} for decolourisation of four structurally different cationic/anionic dyes through simultaneous adsorption and photocatalysis under visible light irradiation was assessed. Under identical conditions, the photocatalytic efficiency of the ZnAl-PW_{12} catalyst was found to be much higher than that of calcined ZnAl-LDH, indicating the promoting effect of $PW_{12}O_{40}^{3-}$ ion. Moreover, the loss of costly polyoxometallate (POM) could be avoided by intercalating the POM ion in the interlayer of LDH, which can facilitate the use of synthesized catalysts for repeated cycles.

Keywords
Polyoxometallate; LDHs; adsorption; photocatalysis; dye decolourisation

1. Introduction

Layered double hydroxides (LDHs) having the general formula $[M^{2+}_{1-x}M^{3+}_{x}(OH)_2]^{x+}(A^{m-}_{x/m})\cdot nH_2O$ form a promising class of materials having numerous technological application competence owing to their particular lamellar structure with many possible combinations of M^{2+} and M^{3+} metal ions as host layer cations, and intercalating anions (A^{m-}) [1-3]. The host layer provides flexible confined space for accommodating a variety of catalytically active organic, polymeric, and inorganic species, resulting in numerous intercalated composite materials with improved chemical properties for the specific application. In this regard, the polyoxometalates intercalated layered double hydroxide hybrid materials have invoked much research interest in recent years due to their distinctive properties and exhibiting advantages over both parent materials, especially in catalytic applications [3-7].

POMs are anionic metal oxides of groups V and VI that constitute a potentially important class of inorganic materials because of their unique properties in terms of structural stability, tunable acidity, redox capability, and catalytic efficiency for various organic transformations in homo- and heterogeneous media besides application potential in other areas such as medicine, pharmaceutical, electronics, etc. [8-10]. The photocatalytic properties of POMs have also been explored for different reactions including the recovery of metals by reducing their ions from aqueous solutions, oxidation of water, removal of CO_2 to CH_4, etc. [11-15]. However, the weak hydrolytic stability and poor recyclability due to high solubility in water seriously restrict their applications for reactions carried out in an aqueous medium. To overcome these limitations, the POMs are often immobilized on appropriate supports for easy recovery from the reactant solution after the reaction. The separated catalyst can be regenerated and reused for further cycles of reaction. Relatively higher activity of immobilized POMs has often been compared to either POM or support alone due to synergistic effects between LDHs and POMs.

In recent decades, significant progress has been made in developing POMs-LDHs materials demonstrating superior catalytic performance for different reactions [16-18]. The photocatalytic activity of POM intercalated LDH is, however, sparsely studied [19-22], although catalytic systems like POMs/TiO_2 showed relatively higher photocatalytic degradation abilities towards aqueous organic pollutants, including dyes, than those of either neat POMs or TiO_2 alone [22-25]. More studies are needed with POM intercalated LDH to identify the effective POMs, optimization of intercalation process, and optimization of catalytic parameters for their possible utilization in the remediation process of dyes.

Herein we report the intercalation of a photoactive POM, tungstophosphate ($PW_{12}O_{40}^{3-}$), in the interlayer of ZnAl-LDH, characterization by different techniques and adsorptive/photocatalytic decolorisation of four structurally different organic dyes under visible light irradiation.

2. Materials and Methods

Analar grade zinc nitrate, $Zn(NO_3)_2{\cdot}6H_2O$; aluminum nitrate, $Al(NO_3)_3{\cdot}9H_2O$; sodium hydroxide (NaOH) and sodium carbonate (Na_2CO_3), as received from SRL (India), were used for the preparation of LDH precursor. Tungstophosphoric acid ($H_3[PW_{12}O_{40}]$) (Merck) is used for intercalating the tungstophosphate anion ($PW_{12}O_{40}^{3-}$) in the interlayer of LDH. Analar grade organic dyes viz. methyl orange (MO), Congo red (CR), methylene blue (MB), and rhodamine B (RhB) are used to evaluate the photocatalytic activity of the prepared catalyst under visible light irradiation. All other chemicals used were of analytical grades and without further purification.

ZnAl-LDH precursor in carbonate form (ZnAl-LDH-CO_3) is prepared by coprecipitation of mixed aqueous solutions of $Zn(NO_3)_2{\cdot}6H_2O$ and $Al(NO_3)_3{\cdot}9H_2O$ at ambient temperature under low supersaturating conditions (pH ~10) [1, 26]. An aqueous solution of metal nitrates (Zn/Al = 3) was added dropwise to a well-stirred solution of Na_2CO_3 (100 ml 0.01 M). Simultaneously, a mixture of NaOH (2.0 M) and Na_2CO_3 (0.02 M) was added such that the pH of the resulting slurry was maintained at ~10 ± 0.2. After complete addition, the resulting slurry is aged for 12 h at room temperature, washed several times with deionized distilled water by dispersion/centrifugation cycles, and dried overnight at 90°C in an air oven. The small amount of nitrate ions retained in the interlayer of LDH precursor is replaced by carbonate ions by suspending the dried precursors (2 g) in the solutions of Na_2CO_3 (100 ml, 0.20 M) and stirring for 2 h. The carbonate-exchanged solid was washed with water by dispersion/centrifugation cycles and dried overnight at 90°C. The dried LDH precursor was calcined at 450°C for 5 h to convert into mixed metal oxide, ZnAl(O) [1, 26].

The tungstophosphate ion, $PW_{12}O_{40}^{3-}$(PW_{12}) was intercalated in the interlayer of LDH through rehydration of calcined ZnAl-LDH in the presence of $H_3PW_{12}O_{40}$ under the N_2 atmosphere to avoid the entry of CO_2 from the atmosphere. In a typical lot weighed amount of calcined ZnAl-LDH, ZnAl(O) was dispersed in 100 ml of water containing the desired amount of $H_3[PW_{12}O_{40}]$, and the pH value was adjusted to ~4.5, which is well within the range of pH (2 to 6) where the POM anion is stable as $PW_{12}O_{40}^{3-}$, The mixture was stirred under N_2 atmosphere for 8 h. The resulting solid was separated by centrifugation, washed several times with water, and finally ethanol. The isolated solid was dried at 60°C for 8 h in a vacuum and stored in a desiccator over silica gel. The sample thus prepared was denoted as ZnAl-PW_{12}.

The Zn, Al, and W contents in the samples were determined by ICP (Varian Liberty series 2). Powder X-ray diffraction patterns were recorded in a Rigaku (Miniflex II) X-ray diffractometer using Ni-filtered CuK_α (30 kV, 15 mA) radiation source. Thermogravimetric measurements in the argon atmosphere were performed on a Shimadzu DTG 60 Thermal analyzer at a heating rate of 10°C/min. FT-IR spectra in KBr phase were recorded on a Shimadzu IR Affinity-1 spectrophotometer averaging 45 scans with a nominal resolution of 4 cm^{-1} to improve the signal-to-noise ratio. The UV-visible diffuse reflectance spectra (UV-Vis DRS) were recorded on a Varian UV-visible spectrophotometer using $BaSO_4$ white standard. The surface areas were measured using a Smart Sorb 92/93 surface area analyzer. The samples were degassed at 100°C for 4 h before analysis.

The photocatalytic activity of the ZnAl-PW_{12} is tested in a double-walled cylindrical glass photoreactor fitted with a 125 W high-pressure Hg lamp and a cut-off filter to eliminate light of wavelength <400 nm. In typical lots, 100 ml of different dye solutions in varying concentrations were treated with a certain amount of catalyst and irradiated with visible light under the stirring condition to initiate the photodegradation. A solution of $NaNO_2$ (1.0 M) was circulated through the outer

jacket of the photoreactor to cut off the light with wavelengths less than 400 nm. At regular intervals, 5.0 ml of the reaction mixture was pipetted out and centrifuged to separate the catalyst and the absorbance of the supernatant solution at the pre-set wavelengths (λ_{max} of different dyes). The concentration of dye was calculated from the estimated absorbance value as per Eq. 1. Each catalytic run was made at least in duplicate and the average value was reported.

$$\%\ \text{of Dye degraded} = [(C_0 - C_t)/C_0] \times 100 \quad (1)$$

Where C_0 is the initial dye concentration, and C_t corresponds to the attention of dye at time t. To see the amount of paint removed from the solution due to adsorption only, batch adsorption experiments were performed by taking 100 ml of dye solution of the desired concentration with the catalyst and stirring for 4 h without the passage of visible light.

3. Results and Discussion

3.1 Characterizations of ZnAl-PW_{12}

The molar ratio of Zn:Al:W in ZnAl-PW_{12} is found to be 0.742:0.267:0.798, indicating all the interlayer charge is not compensated by $PW_{12}O_{40}^{3-}$ ion. About 80% of the interlayer amount of LDH is balanced by $PW_{12}O_{40}^{3-}$ while the remaining amount is balanced by CO_3^{2-} or OH^- ions. Powder XRD patterns of ZnAl-PW_{12}, along with the ZnAl-LDH precursor used for the intercalation of $PW_{12}O_{40}^{3-}$ are shown in Figure 1.

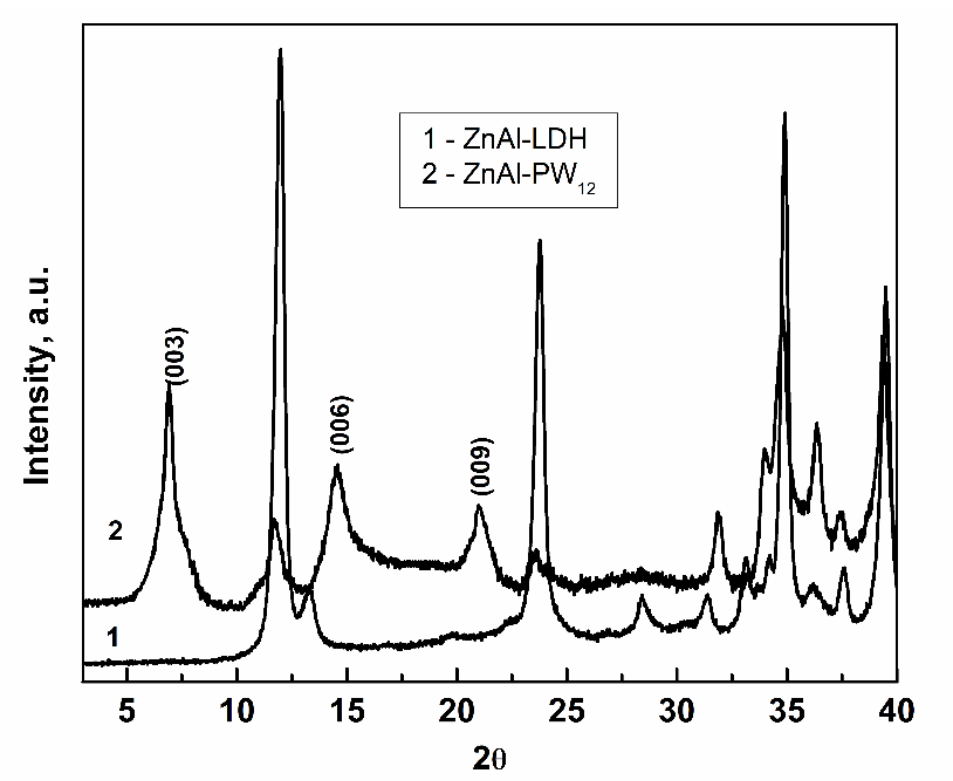

Figure 1 XRD patterns of ZnAl-LDH (1) and $PW_{12}O_{40}^{3-}$ intercalated ZnAl-LDH (2).

The shifting of peaks corresponding to (003), (006), and (009) planes towards lower 2θ values in the case of ZnAl-PW_{12} clearly indicates an expansion of the interlayer space due to intercalation of

ZnW_{12} in the interlayer [1]. Assuming the diameter of Keggin-ion is *ca.* 8 Å and the brucite-like layer thickness 4.8 Å, the calculated basal spacing should be 12.8 Å. Using the 2θ value of (003) reflection, the d_{003} is found to be 12.73 Å, which is well within the range of values reported in the cases of POM intercalated LDHs [1, 17-19]. The XRD pattern with the broad spread of reflections in the case of ZnAl-PW_{12} indicates poor crystallinity due to some structural disorder with the entry of more than one intercalating species (e.g. PW_{12} and OH^-/CO_3^{2-}) into the interlayer region of LDH.

The FT-IR spectra of ZnAl-PW_{12}, $H_3[PW_{12}O_{40}]$ and Zn(Al)O precursor, are shown in Figure 2. The observed broad and intense band between 3600 and 3200 cm^{-1} in all the samples is attributed to –OH stretching from the metal hydroxide and interlayer water. FT-IR of PW_{12} displayed four characteristic vibrational bands arising from P–O bonds of the PO_4 units, W=O bonds, and two W–O–W bonds of the Keggin unit at 1080, 987, 895 and 818 cm^{-1}, respectively [19, 27]. These bands also appeared in the case of ZnAl-PW_{12} with reduced intensities, indicating the existence of PW_{12} in the interlayer of LDH. The characteristic peak for CO_3^{2-} ion at ~1380 cm^{-1} also appeared in the spectrum of ZnAl-PW_{12}, indicating that a small amount of CO_3^{2-} ions has entered during the intercalation process or remained in the calcined ZnAl-LDH. The appearance of low-intensity peaks in the XRD pattern of ZnAl-PW_{12} at the same 2θ values as that of ZnAl-LDH also supported this fact.

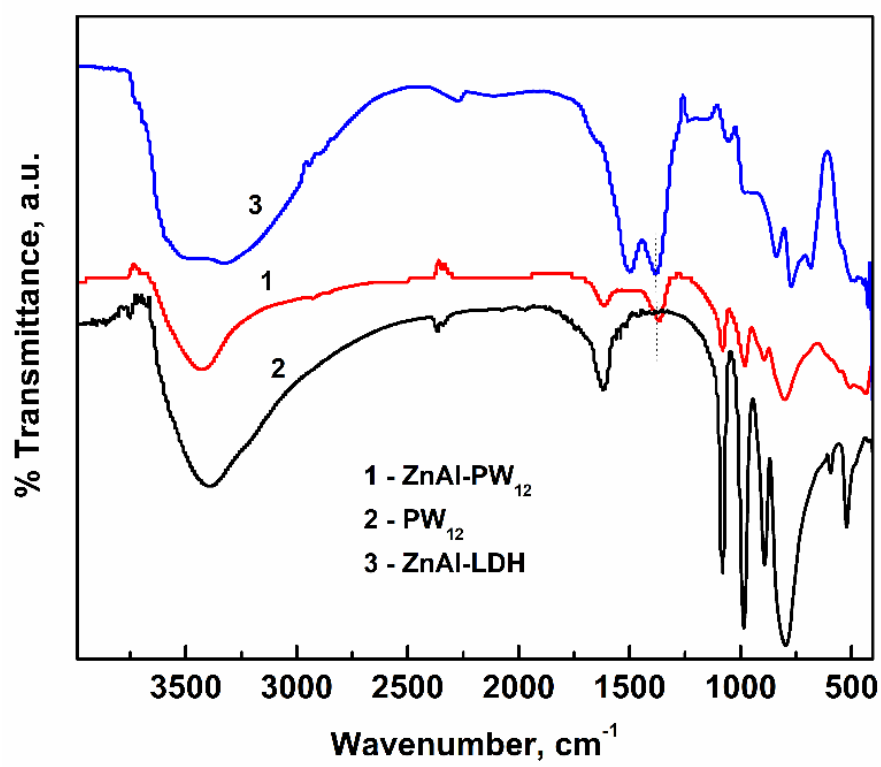

Figure 2 FT-IR spectra of ZnAl-PW_{12} along with pure $PW_{12}O_{40}^{3-}$ and ZnAl-LDH.

The UV-Vis DR spectra of ZnAl-PW_{12} along with PW_{12}, Zn(Al)O, and ZnAl-LDH were shown in Figure 3. The appearance of characteristic peaks of $PW_{12}O_{40}^{3-}$, at ~260 and 340 nm, in the spectra of ZnAl-PW_{12} provided additional evidence in favor of the intercalation of $PW_{12}O_{40}^{3-}$ in the interlayer of reconstructed LDH. More interestingly, the absorption of ZnAl-PW_{12} extends beyond 400 nm, presumably due to the narrowing down of the band gap. The band gap of ZnAl-PW_{12} (2.86 eV) is found to be marginally lower than that of either PW_{12} (3.05 eV) or Zn(Al)O (3.00 eV). The lowering

of band gap from 3.51 eV to 3.10 eV has also been reported for $H_3PW_{12}O_{40}/TiO_2$ composite than that of pure TiO_2 with the increase of $H_3PW_{12}O_{40}$ loadings from 0 to 16.7% [24].

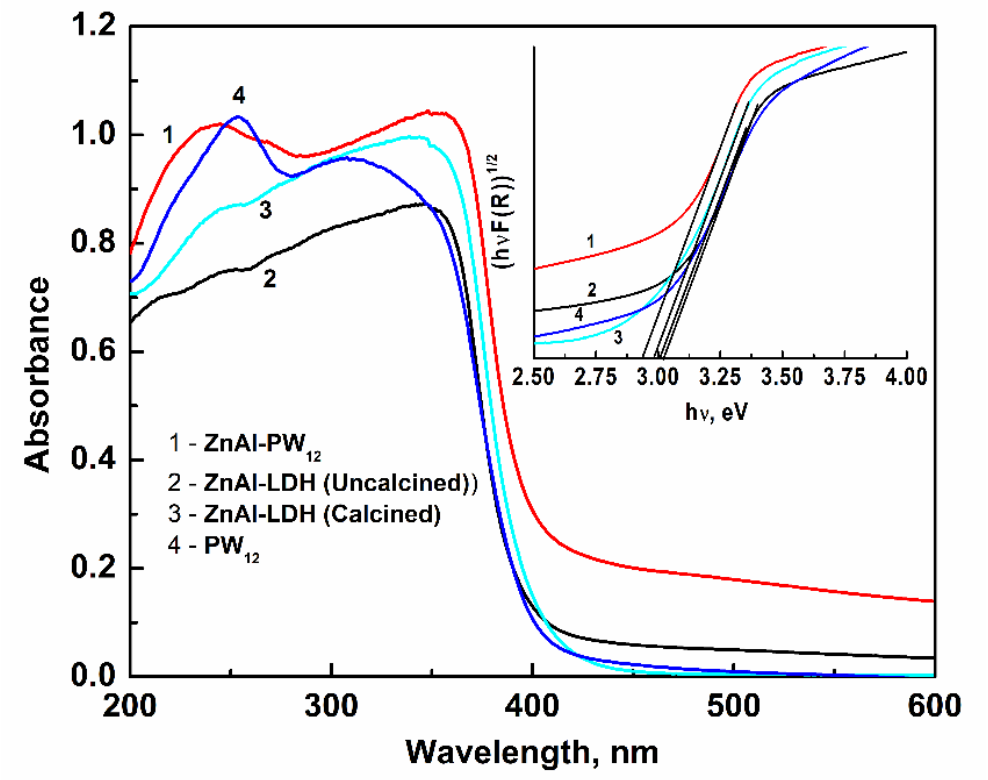

Figure 3 UV-Vis diffuse reflectance spectra of ZnAl-PW_{12} along with pure $PW_{12}O_{40}^{3-}$, unclaimed and calcined ZnAl-LDH [Zn(Al)O].

3.2 Photocatalytic Activity of ZnAl-PW_{12}

The photocatalytic efficiency of ZnAl-PW_{12}, along with ZnAl-LDH, was assessed for degradation of structurally different cationic and anionic dyes in aqueous solutions under visible light irradiation ($\lambda > 400$ nm). The results obtained were discussed below.

3.2.1 Decolourisation of Methyl Orange (MO)

The representative time course degradation of MO under visible light irradiation is presented in Figure 4. The Spectral scan of MO at different intervals during a photocatalytic run (Inset, Figure 4) clearly showed the decrease of absorbance in the entire spectral range without any noticeable change or shift in the peak positions. The initial concentration of MO in all cases was kept within 10^{-4} M (32.7 mg/L) to avoid its dimerization to obey Beer–Lambert's law [28]. A blank test without the photocatalyst showed about 5% degradation of CR throughout 3 h. As evident from Figure 4, MO is significantly removed (~72%, 43.2 mg/g) by Zn(Al)O within 180 min, primarily due to the adsorption/ion exchange of MO. Under identical conditions, only ~12% of MO is removed through adsorption/ion exchange in the case of ZnAl-PW_{12}.

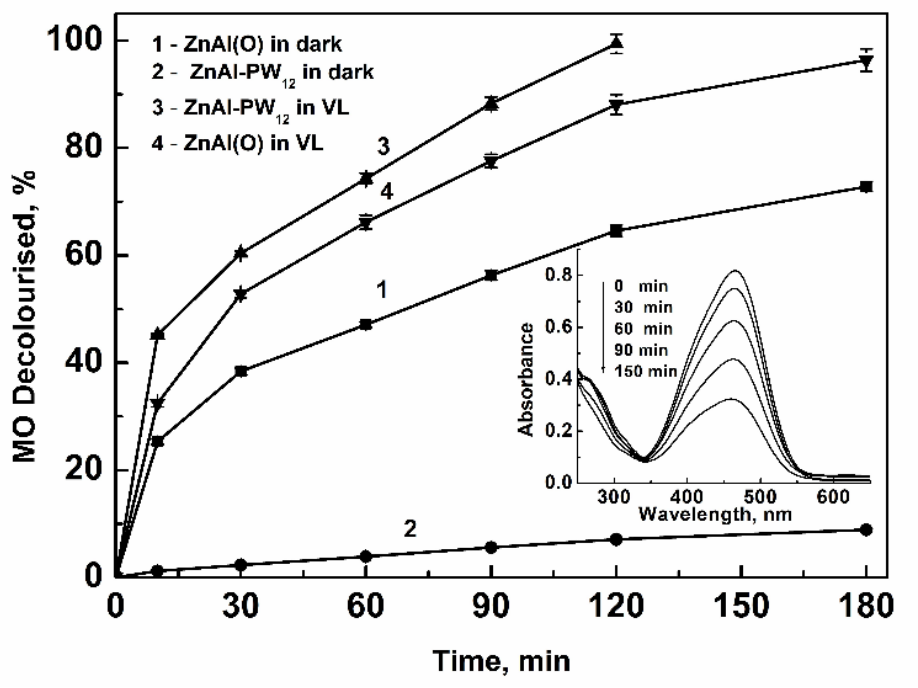

Figure 4 Comparative adsorptive/photocatalytic decolourisation of methyl orange (MO) by Zn(Al)O and ZnAl-PW_{12}; [MO] = 30 mg/L, pH = 5.5 ± 0.03, catalyst = 0.5 g/L. (Inset) successive spectral scan for photocatalytic degradation of MO using ZnAl-PW_{12} (initial MO, 50 mg/L, catalyst dose, 0.50 g/L).

The lower percentage of MO removal, in this case, is obviously due to (i) the competition from existing interlayer anions ($PW_{12}/CO_3^{2-}/OH^-$) for its entry in the anionic form and (ii) presence of the relatively lesser amount of charge balancing interlayer anionic sites available for MO with the same wt. (0.5 g/l) of ZnAl-PW_{12}. Hence, the overall removal of MO by Zn(Al)O is mainly due to the entry of MO in the interlayer through rehydration, while more than 98% of total MO (30 mg/l) removal within 120 min in the case of ZnAl-PW_{12} mainly results from its photocatalytic degradation under visible light. The decolorisation data were fitted to the first-order equation, and the rate constant with 30 mg/l (initial concentration) was found to be 2.14×10^{-2} s^{-1}. The results of overall MO decolorisation at varying initial MO concentrations and catalyst doses are presented in Figure S1. The overall MO decolorisation increases linearly with an increase in catalyst dose at the beginning and then nonlinearly at a higher dose of catalyst, presumably due to the turbidity of the suspended catalyst that shields the penetration of visible light. On the other hand, a progressive decrease in the overall decolorisation of MO is observed with the increase of MO concentration due to decreased active sites on the catalyst surface for MO adsorption, followed by its degradation. It may be noted that the final pH in each case is increased at the end of the photocatalytic run, and the pH values vary in the range of 6.7 to 7.5.

3.2.2 Decolourisation of Congo Red (CR)

The results of CR decolorisation, both in the presence and absence of visible light, are depicted in Figure 5. The corresponding spectral change (inset, Figure 5) over the reaction period in the presence of light shows a decrease in absorbance without any noticeable shift in the peak positions.

CR, like MO, also exists in the anionic form at pH ~6.2 (pK_a of CR ~3.0-5.0) and can enter the interlayer of LDH during the photocatalytic run.

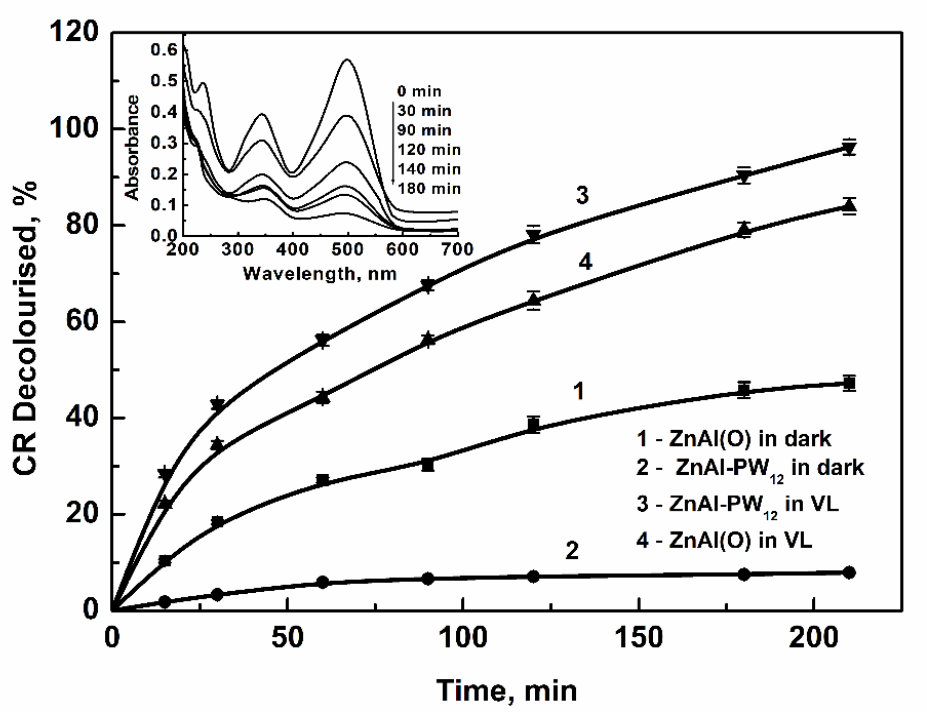

Figure 5 Comparative adsorptive/photocatalytic decolourisation of Congo red (CR) by Zn(Al)O and ZnAl-PW_{12}; (initial [CR], 50 mg/l, pH ~6.2, catalyst 0.5 g/l). (Inset) Successive UV-Vis spectra of CR during its decolourisation by ZnAl-PW_{12} under visible light irradiation ([CR], 50 mg/l, pH ~6.2).

It is seen that ~45% of CR was removed by Zn(Al)O without light through adsorption or exchange in the interlayer of rehydrated Zn(Al)O, which is relatively less than that observed in the case of MO (72%) presumably due to bigger molecular size of CR than MO. In comparison, only 8-10% CR is removed (without light) by ZnAl-PW_{12}. The removal (decolorisation) of CR is significantly increased on light irradiation, indicating the promotional effect of PW_{12} in the interlayer of ZnAl-PW_{12}. About 80% of CR (50 mg/L) is decolorised within 120 min under visible light irradiation with a rate constant of 1.41×10^{-2} s^{-1}. The results of CR decolorisation under varying initial concentrations and catalyst doses were presented in Figure S2. As expected, the overall decolorisation of CR was found to decrease with the increase of initial CR concentration and a decrease of catalyst dose similar to that observed in the case of MO.

3.2.3 Decolourisation of Methylene Blue (MB)

Comparative efficiency of Zn(Al)O and ZnAl-PW_{12} towards the removal of MB is presented in Figure 6, along with spectral change during a typical photocatalytic run. It is seen that the initial peaks at 614 and 664 nm are merged into a relatively broad peak, centered at ~650 nm, during the reaction, and the peak intensities are also reduced progressively with a shift towards higher wavelengths till the reactant solution turns colorless [29]. On the other hand, the powers of MB bands at 292 and 245 nm are reduced progressively without any shift in their positions. The

disappearance of two major absorbance peaks of MB at 292 and 664 nm, due to benzene ring and heteropolyaromatic linkage, indicate their destruction at the end of the reaction [29].

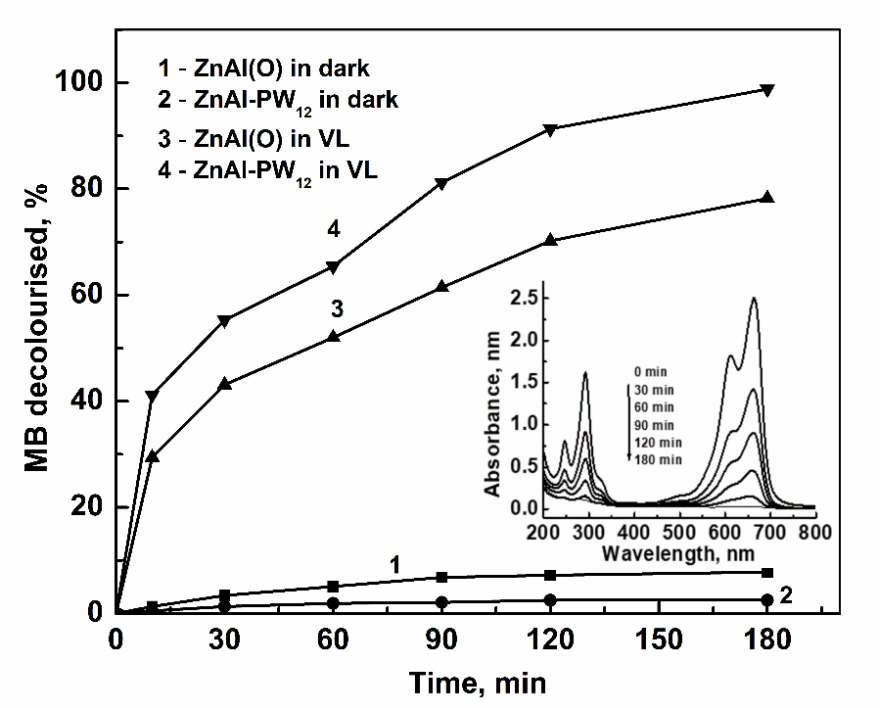

Figure 6 Comparative adsorptive/photocatalytic decolourisation of methylene blue (MB) by Zn(Al)O and ZnAl-PW_{12}; (MB, 50 mg/l, pH ~6.2, catalyst, 0.5 g/l). (Inset) UV-Vis spectra showing progressive decolourisation of MB using ZnAl-PW_{12} under visible light irradiation (MB, 50 mg/l, pH ~6.2, catalyst, 0.5 g/l).

In comparison to MO, the removal of MB by either Zn(Al)O or ZnAl-PW_{12} in the dark condition is much lower as MB exists in the cationic form at pH ~6.2 (pKa > 12), and therefore, removal of MB is primarily due to its adsorption on the LDH surface by electrostatic interaction. It is seen that ZnAl-PW_{12} shows relatively higher activity than the Zn(Al)O throughout the reaction period, indicating the promoting photocatalytic effect of intercalated POM. Like other dyes, the percentage of MB decolorisation is also found to increase with the increase of catalyst dose and a decrease of initial MB concentration (Figure S3). Complete degradation of MB (50 mg/L) is observed in 120 min of irradiation with a catalyst dose of 1.0 g/L with a rate constant of 2.25×10^{-2} s^{-1}.

3.2.4 Decolourisation of Rhodamine B (RhB)

Another cationic dye, rhodamine B (RhB), was selected to assess the photocatalytic potential of ZnAl-PW_{12} due to its absorption in the visible-light region and excellent stability over a wide range of pH. The decolorisation of RhB is evident from the significant decrease in absorbance change during the photocatalytic reaction without any significant shift in the peak positions (Figure 7, inset), indicating the decolorisation of RhB is primarily due to the decomposition of conjugated chromophore structure rather than de-ethylation process [30]. To avoid the colour change due to pH variation, the photocatalytic reaction was carried out at pH (~6.2), much above the pK_a of RhB (= 3.7), where it mainly exists in zwitterionic form due to deprotonation of the carboxyl group. Like

MB, the removal of RhB in the absence of light by adsorptions over ZnAl-PW_{12} or ZnAl(O) is relatively low, ~5.3% and 9.2%, respectively (Figure 7).

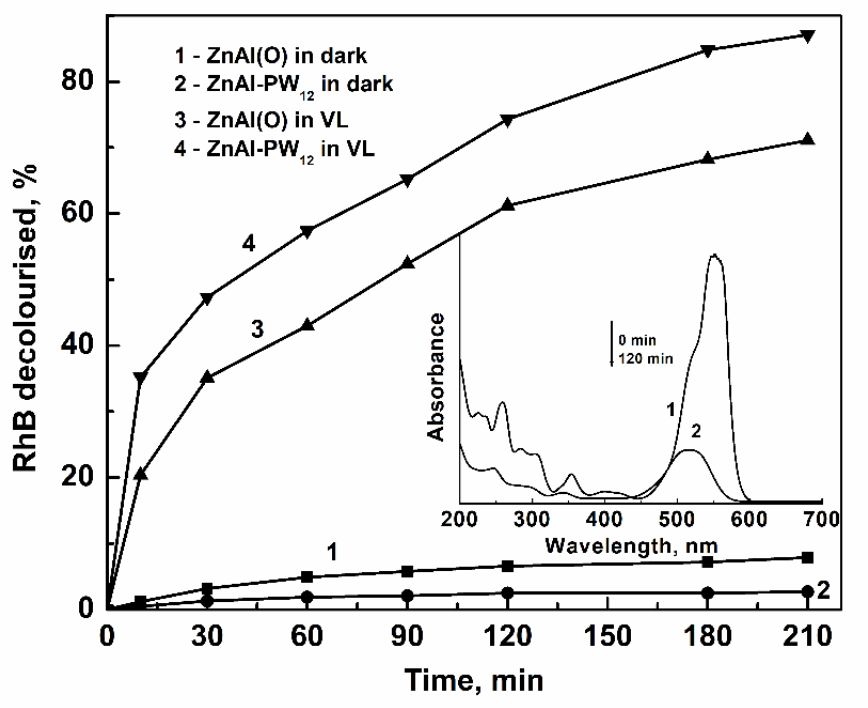

Figure 7 Comparative adsorptive/photocatalytic decolourisation of Rhodamine B (RhB) by Zn(Al)O and ZnAl-PW_{12}; (RhB, 30 mg/l, pH ~6.2, catalyst, 0.5 g/l). (Inset) Successive spectral scan of RhB during its decolourisation by ZnAl-PW_{12} under visible light irradiation at pH ~6.2.

The catalytic effect of PW_{12} (in ZnAl-PW_{12}) over ZnAl(O) is also evident from the figure. Figure S4 presents the impact of catalyst dose and initial dye concentration, similar to those obtained for other dyes. In a recent study, the enhanced photocatalytic effect of $H_3PW_{12}O_{40}/TiO_2$ composite films with different $H_3PW_{12}O_{40}$ loadings (6.3, 7.7, 14.7 and 16.7%) has been seen towards degradation and mineralization of an aqueous dye RhB under solar simulating Xe lamp irradiation ($320 < \lambda, nm < 780$) [31]. Complete degradation of RhB (25 mg/L) has been observed in 120 min with a catalyst dose of only 45 mg/l. In comparison, about 86.6% of RhB (30 mg/l) is degraded in 210 min with a catalyst dose of 1.0 g/l in the present case due to different amounts of PW_{12} loading. The decolourisation data was fitted well to the first order equation, and the rate constant with 30 mg/l (initial concentration) was found to be 8.9×10^{-3} s^{-1}. The overall decolorisation of RhB is also found to decrease with the increase of initial RhB concentration and decrease of catalyst dose similar to that observed in the cases of other dyes.

3.3 Comparative Photocatalytic Activity and Probable Mechanism

The photocatalytic efficiencies of some related photocatalysts for degradation/decolourisation of different organic dyes were presented in Table 1, along with those observed in this work. It is worth noting that ZnAl-PW_{12} efficiently decolourises several shades under visible irradiation with comparable activity as those of other photocatalysts [27, 31-36].

Table 1 Comparative activity of some relevant catalysts towards decolourisation of different organic dyes.

Catalytic systems	Light source	Dyes	Reaction conditions	Conversion %	Refs.
			Dye conc. (mg/L), pH, catalyst (g/L), reaction time (min)		
$PW_{12}O_{40}^{3-}/SiO_2$	SS[2]	MO	10.0, 2.5, 2.0, 210	~35	[32]
$PW_{12}O_{40}^{3-}/SiO_2$ (H_2O_2 treated)	SS[2]	MO	10.0, 2.5, 2.0, 210	~95	[32]
$SiW_{12}O_{40}^{4-}$/Cucubi[6]uril	Vis	MO	10.0, 2.5, 0.5, 120	93.6	[33]
$H_3SiW_{12}O_{40}^{4-}$ (Powder)	UV	MO	10, __, 1.0, 30	4.6	[34]
$H_3SiW_{12}O_{40}^{4-}$	Vis	RhB	10, __, 1.0, 480	45	[35]
$H_3SiW_{12}O_{40}$/PVA	Vis	RhB	10, __, 1.0, 480	74	[35]
$H_3SiW_{12}O_{40}$/PVA/Ag	Vis	RhB	10, __, 1.0, 480	100	[35]
$H_3PW_{12}O_{40}$ (14.7wt.%)/TiO_2	SS[2]	RhB	25, 3-4, 0.0375, 180	92	[31]
$PW_{12}O_{40}^{4-}$/Resin	Vis (>450 nm)	RhB	9.58, 2.5, 0.06, 240	95	[27]
$SiW_{12}O_{40}^{4-}$/MAC/HMT[1]	Solar/Vis./UV	MB	40.0, --, 0.44, 75	94.9/91.9/92.7	[36]
$PW_{12}O_{40}^{3-}$/ZnAl-LDH	Vis (>400 nm)	MO	30.0, 5.5, 0.5, 120	98.4	This work
	Vis (>400 nm)	CR	50.0, 6.2, 0.5, 120	80.2	This work
	Vis (>400 nm)	MB	50.0, 6.2, 0.5, 120	99.2	This work
	Vis (>400 nm)	RhB	30.0, 6.2, 0.5, 120	86.6	This work

[1]MAC = Magnetic activated carbon, HMT = Hexamethylene tetraamine; [2]SS = Simulated sunlight

The photocatalytic decolourisation/degradation of dyes by semiconducting oxides occurs most likely either through (i) photoexcitation of oxide leading to the electron/hole pairs on its surface followed by the formation of hydroxide radical ($HO^{\bullet}$) by the decomposition of the water or by reaction of the holes with HO^- and its response with dye molecules to yield the degradation products as delineated in Eqs. (2 to 5).

$$\text{Catalyst} + h\nu \rightarrow \text{Catalyst}\ (e^-_{CB} + h^+_{VB}) \quad (2)$$

$$H_2O + h^+_{VB} \rightarrow H^+ + OH^{\bullet} \quad (3)$$

$$HO^- + h^+_{VB} \rightarrow HO^{\bullet} \quad (4)$$

$$HO^{\bullet} + \text{Dye} \rightarrow \text{degradation products} \quad (5)$$

and/or (ii) absorption of visible light catalyst/Dye system leading to excitation of the surface-adsorbed dye molecule (Eq. 6), which affects the charge transition into the conduction band of catalyst in the excited state (Eq. 7). The electron in the conduction band (e^-_{CB}) is then transferred to molecular oxygen, leading to the formation of a series of radicals capable of decolorising/degrading the dye molecules.

Since the measured band gap of ZnAl-PW_{12} is relatively high (3.02 eV), the mechanism of dye degradation based on generation (e^-/h^+) pairs under visible light irradiation is less likely, although not completely ruled out. Alternatively, a photosensitized pathway with light absorption, mainly

through dye molecule adsorbed/exchanged on the catalyst surface (ZnAl-PW_{12}/Dye), leads to excitation of the surface-adsorbed dye molecule (Eq. 6), which affects the charge transition into ZnAl-PW_{12} conduction band (Eq. 7). The excited dye molecule undergoes degradation (Eq. 8). In addition, the electron from the conduction band (e^-_{CB}) is combined with the molecular oxygen yielding a series of radicals capable of decolourising/degrading of the dye molecule (Eqs. 9-14). The overall photocatalytic process may be delineated as follows:

$$\mathrm{ZnAl-PW_{12}/Dye + h\nu \rightarrow ZnAl-PW_{12}/Dye*} \quad (6)$$

$$\mathrm{ZnAl-PW_{12}/Dye* \rightarrow ZnAl-PW_{12}\,(e^-_{CB})/Dye^{+\bullet}} \quad (7)$$

$$\mathrm{Dye^{+\bullet} \rightarrow degradation\ products} \quad (8)$$

$$\mathrm{ZnAl-PW_{12}\,(e^-_{CB}) + O_2 \rightarrow ZnAl-PW_{12} + O_2^{-\bullet}} \quad (9)$$

$$\mathrm{H_2O + O_2^{-\bullet} \rightarrow HOO^{\bullet}} \quad (10)$$

$$\mathrm{HOO^{\bullet} + H_2O + e^-_{CB} \rightarrow H_2O_2 + OH^- \rightarrow HO^{\bullet} + OH^-} \quad (11)$$

$$\mathrm{H_2O_2 + O_2^{-\bullet} \rightarrow HO^{\bullet} + OH^- + O_2} \quad (12)$$

$$\mathrm{Dye^{+\bullet} + O_2^{-\bullet} \rightarrow Dye-O_2 \rightarrow degradation\ products} \quad (13)$$

$$\mathrm{HO^{\bullet}/O_2^{-\bullet} + Dye \rightarrow degradation\ products} \quad (14)$$

4. Conclusions

Tungstophosphate ($PW_{12}O_{40}^{3-}$) is efficiently intercalated between the layers of three-dimensionally ordered ZnAl-LDH through rehydration of calcined ZnAl-LDH (Zn/Al ~3.0) under N_2 atmosphere. The chemical analyses coupled with characterization by PXRD, FT-IR, and DR/UV-Vis spectra of the as-prepared intercalated sample (ZnAl-PW_{12}) and their comparison with pure $H_3PW_{12}O_{40}$ indicated about 80% of the residual positive charge in the brucite layer was balanced by $PW_{12}O_{40}^{3-}$.

The photocatalytic properties of ZnAl-PW_{12} were evaluated using decolorisation of some model anionic (methyl orange and Congo red) and cationic (methylene blue and rhodamine B) under visible light irradiation. Decolorisation of dyes was evident from a progressive decrease of absorbance in their successive UV-Visible spectral scan during the photocatalytic runs. In all the cases, the extent of dye decolourisation increased with an increase in catalyst doses or a decrease in initial dye concentrations. Under identical conditions and without light irradiation, the adsorption/exchange of dyes on ZnAl-PW_{12} is significantly lower than that of calcined ZnAl-LDH [ZnAl(O)]. On the other hand, in the presence of light, the adsorptive/photo-decolorisation by ZnAl-PW_{12} was significantly higher than that shown by ZnAl(O), indicating the promoting effect of PW_{12}. In summary, the present study demonstrated that PW_{12} intercalated LDH promises to be an excellent photocatalytic system for many practical applications. Moreover, the intercalation of PW_{12} in the interlayer of LDH avoided the loss of costly PW12 and increased the photocatalytic activity.

Acknowledgements

The authors acknowledged the Department of Chemistry, Utkal University for extending the facilities for carrying out the work.

Author Contributions

B. S. Mohanta: Synthesis of materials, data collections, and compilation; R. Das: Experiment design, data analysis, finalization of the manuscript; N. Das: Experiment design, data analysis, rough draft, and finalization of the manuscript.

Competing Interests

The authors have declared that no competing interests exist.

Additional Materials

The following additional materials are uploaded at the page of this paper.

1. Figure S1: Effect of concentration of dye and wt. of catalyst (ZnAl-PW_{12}) towards adsorptive/photocatalytic decolourisation of methyl orange (MO).
2. Figure S2: Effect of concentration of dye and wt. of catalyst (ZnAl-PW_{12}) towards adsorptive/photocatalytic decolourisation of Congo red (CR).
3. Figure S3: Effect of concentration of dye and wt. of catalyst (ZnAl-PW_{12}) towards adsorptive/photocatalytic decolourisation of methylene blue (MB).
4. Figure S4: Effect of concentration of dye and wt. of catalyst (ZnAl-PW_{12}) towards adsorptive/photocatalytic decolourisation of Rhodamine B (RhB).

References

1. Cavani F, Trifiro F, Vaccari A. Hydrotalcite-type anionic clays: Preparation, properties and applications. Catal Today. 1991; 11: 173-301.
2. Baskaran T, Christopher J, Sakthivel A. Progress on layered hydrotalcite (HT) materials as potential support and catalytic materials. RSC Adv. 2015; 5: 98853-98875.
3. Li T, Miras HN, Song YF. Polyoxometalate (POM)-Layered Double Hydroxides (LDH) composite materials: Design and catalytic applications. Catalysts. 2017; 7: 260.
4. Rives V, Ulibarri MA. Layered double hydroxides (LDH) intercalated with metal coordination compounds and oxometalates. Coord Chem Rev. 1999; 181: 61-120.
5. Omwoma S, Chen W, Tsunashima R, Song YF. Recent advances on polyoxometalates intercalated layered double hydroxides: From synthetic approaches to functional material applications. Coord Chem Rev. 2014; 258: 58-71.
6. Han Q, Ding Y. Recent advances in the field of light-driven water oxidation catalyzed by transition-metal substituted polyoxometalates. Dalton Trans. 2018; 47: 8180-8188.
7. Patel A, Narkhede N, Singh S, Pathan S. Keggin-type lacunary and transition metal substituted polyoxometalates as heterogeneous catalysts: A recent progress. Catal Rev Sci Eng. 2016; 58: 337-370.

8. Mizuno N, Yamaguchi K, Kamata K. Epoxidation of olefins with hydrogen peroxide catalyzed by polyoxometalates. Coord Chem Rev. 2005; 249: 1944-1956.
9. Ghiasi Moaser A, Afkham AG, Khoshnavazi R, Rostamnia S. Nickel substituted polyoxometalates in layered double hydroxides as metal-based nanomaterial of POM–LDH for green catalysis effects. Sci Rep. 2023; 13: 4114.
10. Duarte TA, Estrada AC, Simões MM, Santos IC, Cavaleiro AM, Neves MG, et al. Homogeneous catalytic oxidation of styrene and styrene derivatives with hydrogen peroxide in the presence of transition metal-substituted polyoxotungstates. Catal Sci Technol. 2015; 5: 351-363.
11. Rajeshwar K, Osugi ME, Chanmanee W, Chenthamarakshan CR, Zanoni MV, Kajitvichyanukul P, et al. Heterogeneous photocatalytic treatment of organic dyes in air and aqueous media. J Photochem Photobiol C. 2008; 9: 171-192.
12. Troupis A, Hiskia A, Papaconstantinou E. Selective photocatalytic reduction–recovery of palladium using polyoxometallates. Appl Catal B. 2004; 52: 41-48.
13. Gkika E, Troupis A, Hiskia A, Papaconstantinou E. Photocatalytic reduction of chromium and oxidation of organics by polyoxometalates. Appl Catal B. 2006; 62: 28-34.
14. Xue X, Yu F, Li JG, Bai G, Yuan H, Hou J, et al. Polyoxometalate intercalated NiFe layered double hydroxides for advanced water oxidation. Int J Hydrog Energy. 2020; 45: 1802-1809.
15. Zhang H, Cui D, Shen T, He Tong, Sun D, An S, et al. Engineering of PMo_{12}@NiCo-LDH composite via in situ encapsulation-reassembly strategy for highly selective photocatalytic reduction of CO_2 to CH_4. Inorg Chem Front. 2023; 10: 1421-1430.
16. Liu JC, Qi B, Song YF. Engineering polyoxometalate-intercalated layered double hydroxides for catalytic applications. Dalton Trans. 2020; 49: 3934-3941.
17. Stamate AE, Pavel OD, Zavoianu R, Marcu IC. Highlights on the catalytic properties of polyoxometalate-intercalated layered double hydroxides: A review. Catalysts. 2020; 10: 57.
18. Sun X, Dong J, Li Z, Liu H, Jing X, Chi Y, et al. Mono-transition-metal-substituted polyoxometalate intercalated layered double hydroxides for the catalytic decontamination of sulfur mustard simulant. Dalton Trans. 2019; 48: 5285-5291.
19. Xu M, Bi B, Xu B, Sun Z, Xu L. Polyoxometalate-intercalated ZnAlFe-layered double hydroxides for adsorbing removal and photocatalytic degradation of cationic dye. Appl Clay Sci. 2018; 157: 86-91.
20. Mantilla A, Tzompantzi F, Fernández JL, Góngora JD, Mendoza G, Gómez R. Photodegradation of 2,4-dichlorophenoxyacetic acid using ZnAlFe layered double hydroxides as photocatalysts. Catal Today. 2009; 148: 119-123.
21. Lei X, Yang X, Guo Y, Ma F, Guo Y, Yuan Y, et al. Simulated sunlight photodegradation of aqueous phthalate esters catalyzed by the polyoxotungstate/titania nanocomposite. J Hazard Mater. 2010; 178: 1070-1077.
22. Da Silva ES, Prevot V, Forano C, Wong-Wah-Chung P, Burrows HD, Sarakha M. Heterogeneous photocatalytic degradation of pesticides using decatungstate intercalated macroporous layered double hydroxides. Environ Sci Pollut Res. 2014; 21: 11218-11227.
23. Shi H, Zhao T, Zhang Y, Tan H, Shen W, Wang W, et al. Pt/POMs/TiO_2 composite nanofibers with an enhanced visible-light photocatalytic performance for environmental remediation. Dalton Trans. 2019; 48: 13353-13359.

24. Lu N, Zhao Y, Liu H, Guo Y, Yuan X, Xu H, et al. Design of polyoxometallate-titania composite film ($H_3PW_{12}O_{40}/TiO_2$) for the degradation of an aqueous dye Rhodamine B under the simulated sunlight irradiation. J Hazard Mater. 2012; 15: 1-8.
25. Lu N, Wang Y, Ning S, Zhao W, Qian M, Ma Y, et al. Design of plasmonic Ag-$TiO_2/H_3PW_{12}O_{40}$ composite film with enhanced sunlight photocatalytic activity towards o-chlorophenol degradation. Sci Rep. 2017; 7: 17298.
26. Tichit D, Das N, Coq B, Durand R. Preparation of Zr-containing layered double hydroxides and characterization of the acido-basic properties of their mixed oxides. Chem Mater. 2002; 14: 1530-1538.
27. Lei P, Chen C, Yang J, Ma W, Zhao J, Zang L. Degradation of dye pollutants by immobilized polyoxometalate with H_2O_2 under visible-light irradiation. Environ Sci Technol. 2005; 39: 8466-8474.
28. Gould DM, Spiro M, Griffith WP. Mechanism of bleaching by peroxides: Part 5. Kinetics of the peroxide bleaching of crocetin catalysed by $[Co_3^{II}W\{Co^{II}W_9O_{34}\}_2(H_2O)_2]^{12-}$. J Mol Catal A Chem. 2002; 186: 69-77.
29. Sahu RK, Mohanta BS, Das NN. Synthesis, characterization and photocatalytic activity of mixed oxides derived from ZnAlTi ternary layered double hydroxides. J Phys Chem Solids. 2013; 74: 1263-1270.
30. Dong T, Li Z, Ding Z, Wu L, Wang X, Fu X. Characterizations and properties of Eu^{3+}-doped $ZnWO_4$ prepared via a facile self-propagating combustion method. Mater Res Bull. 2008; 43: 1694-1701.
31. Fujimori T, Takaoka M. Thermochemical chlorination of carbon indirectly driven by an unexpected sulfide of copper with inorganic chloride. J Hazard Mater. 2011; 197: 345-351.
32. Huang Y, Yang Z, Yang S, Xu Y. Photodegradation of dye pollutants catalyzed by $H_3PW_{12}O_{40}/SiO_2$ treated with H_2O_2 under simulated solar light irradiation. J Adv Nanomater. 2017; 2: 3.
33. Cao M, Lin J, Lu J, You Y, Liu T, Cao R. Development of a polyoxometallate-based photocatalyst assembled with cucurbit[6]uril via hydrogen bonds for azo dyes degradation. J Hazard Mater. 2011; 186: 948-951.
34. Wang W, Yang S. Photocatalytic degradation of organic dye methyl orange with phosphotungstic acid. J Water Resource Prot. 2010; 2: 979-983.
35. Sui C, Li C, Guo X, Cheng T, Gao Y, Zhou G, et al. Facile synthesis of silver nanoparticles-modified PVA/$H_4SiW_{12}O_{40}$ nanofibers-based electrospinning to enhance photocatalytic activity. Appl Surf Sci. 2012; 258: 7105-7111.
36. Taghdiri M. Selective adsorption and photocatalytic degradation of dyes using polyoxometalate hybrid supported on magnetic activated carbon nanoparticles under sunlight, visible, and UV irradiation. Int J Photoenergy. 2017; 2017: 8575096.